UDK 621.763:67.017:621.7.073 ISSN 1580-2949
Original scientific article/Izvirni znanstveni članek MTAEC9, 50(3)373(2016)

WORKABILITY BEHAVIOUR OF Cu-TiB_2 POWDER-METALLURGY PREFORMS DURING COLD UPSETTING

PREOBLIKOVALNOST Cu-TiB_2 PREDOBLIK IZDELANIH Z METALURGIJO PRAHOV MED HLADNIM KOVALNIM PREIZKUSOM

Saikumar Gadakary[1], Asit Kumar Khanra[1], Maharajan Joseph Davidson[2]

[1]National Institute of Technology, Department of Metallurgical and Materials Engineering, Warangal, India
[2]National Institute of Technology, Department of Mechanical Engineering, Warangal, India
sai.gadakary@gmail.com

Prejem rokopisa – received: 2015-04-07; sprejem za objavo – accepted for publication: 2015-06-17

doi:10.17222/mit.2015.074

An investigation was carried out to find the workability behaviour of a Cu-TiB_2 composite under triaxial stress-state conditions. Initially, the TiB_2 powder was prepared by using a self-propagating high-temperature synthesis (SHS) technique and the same was added to a Cu matrix in order to make Cu-TiB_2 composites. Cylindrical preforms with three different TiB_2 weight percentages (2 %, 4 % and 6 %) with aspect ratios of 0.50, 0.75 and 1 were prepared using a uniaxial load. Then the preforms were pressureless sintered in a tubular furnace with a continuous flow of pure argon gas at 950 °C for a period of 1 h. The cold upsetting test was carried out on the sintered specimens. The relationships between the various stresses, strains and the relative density were determined. The results for the various stress-ratio parameters, namely ($\sigma_\theta/\sigma_{eff}$) and ($\sigma_m/\sigma_{eff}$), the formability stress index (β_σ) under triaxial stress-state conditions were systematically analysed. The formability stress index was found to increase with the increase in preform fractional density and it decreased with the aspect ratios. This was because the preform contains more pores and the porous bed height is high. A statistical fitting method was performed on the curve drawn between the axial strain and the stress-formability index. The compacts with a higher value of the aspect ratio and the initial preform density showed a very high fracture strain.

Keywords: SHS, powder metallurgy, TiB_2, workability, relative density, fracture strain

Izvršena je bila preiskava preoblikovalnosti Cu-TiB_2 kompozita pri triosnem napetostnem stanju. Najprej je bil pripravljen prah TiB2; s pomočjo napredujoče visoko temperaturne sinteze (SHS), ki je bil dodan Cu osnovi, da bi napravili Cu-TiB_2 kompozit. Z enoosnim stiskanjem so bili pripravljeni vzorci cilindrične oblike s tremi različnimi vsebnostmi TiB_2 v masnih deležih (2 %, 4 % and 6 %) in z razmerjem 0,50, 0,75 in 1. Nato so bile predoblike sintrane v cevasti peči pri kontinuirnem pretoku čistega argona na temperaturi 950 °C in trajanju 1 h. Kovni preizkus v hladnem je bil izveden na sintranih vzorcih. Ugotovljena je bila odvisnost med različnimi napetostmi, raztezki in relativne gostote. Sistematično so bili analizirani rezultati različnih parametrov ($\sigma_\theta/\sigma_{eff}$) in ($\sigma_m/\sigma_{eff}$) ter indeks preoblikovalnih napetosti (β_σ) pri triosnem napetostnem stanju. Ugotovljeno je, da indeks preoblikovalne napetosti narašča z naraščanjem gostote predoblike in se zmanjšuje z razmerjem širina-višina. Razlog za to je večje število por v predobliki in zato je višina poroznega vzorca višja. Izvedena je bila tudi statistična obdelava krivulje, narisane med osno napetostjo in indeksom preoblikovalne napetosti. Stiskanci z višjo vrednostjo razmerja med širino in višino ter večjo gostoto predoblike, so pokazali veliko napetost pri porušitvi.

Ključne besede: SHS, metalurgija prahov, TiB_2, preoblikovalnost, relativna gostota, napetost pri porušitvi

1 INTRODUCTION

Powder metallurgy (P/M) is one of the most actively researched manufacturing processes capable of delivering near-net-shaped precision metal parts. This process has delivered a large number of industrial components, such as connecting rods in engines, self-lubricating bearings, gear sets in automobile transmissions, etc.[1–2] Near-net-shape components can be made and, the process has the capability to greatly reduce machining costs, and can improve material utilization.[3–4] A series of upsetting, bending, rolling and plane strain tests to assess the fracture behaviour of porous materials was carried out.[5] P/M components involving copper are a highly researched composite materials as alloys with copper as one of the constituents will be stronger and durable.[6-8]

Copper P/M parts are used extensively in both structural and non-structural applications because of the high corrosion resistance, high thermal and electrical conductivity. The corrosion resistance can be further improved by the application of chemical conversion coatings or anodizing treatment. In general, the physical and mechanical properties of near-full (theoretical) density copper and copper alloy P/M structural parts are comparable to cast and wrought copper-based materials of a similar composition. However, P/M copper parts vary in density from the low-density self-lubricating bearings or filters to the near-full density of the electrical parts.

TiB_2, due to its high melting temperature, hardness, elastic modulus, electro-conductibility and thermal diffusivity, and excellent refractory properties and chemical inertness has been widely used in many industrial fields. It has applications in rocket nose cones for atmospheric re-entry, ballistic armour, cathodes for Hall-Heroult cells, crucibles for molten metals, metal evaporation boats, and as acoating on cutting tools.[9–10] It is widely used as cutting-tool composites and wear-resistant parts.[11] The TiB_2 powder is synthesized using the SHS method. The main feature of the SHS process is that, it utilizes the high energy released during the exothermic chemical reaction of the reactants to yield a variety of inorganic materials. Once the reactants are ignited by an external source, the reaction front propagates within the solid with a certain velocity to complete the chemical reaction.

The extent of deformation possible without failure is defined by the term "workability". It is the ability of a material to withstand the induced internal stresses of forming before any failure occurs. It is the extent to which a material can be deformed in a specific metal working process without the initiation of cracks.[12–14] Workability depends on both the material and the process parameters. The workability of dense material is better than with P/M material. The workability can be calculated by interpreting the value of hydrostatic stress and effective stress for a tri-axial state of compression, and the hydrostatic stress can be evaluated from the axial and hoop stresses. The evaluation of different stresses and the failure strain will reveal the workability limits of the P/M composites.[15] M. Abdel-Rahman and E. Sheikh[16] explored the effect of the relative density on the forming limit of P/M compacts during upsetting. J. J. Park et al.[17] developed a constitutive relation involving the Poisson's ratio, relative density and flow stress to predict the plastic deformation behaviour of porous metals. A mathematical equation for the calculation of the flow stress in the case of a simple upsetting of P/M sintered performs was proposed by R. Narayanasamy et al.[18] Furthermore, the authors developed a new equation for the determination of the hydrostatic stress in the case of the simple upsetting of sintered P/M compacts. Equations for the determination of the flow stress and the hydrostatic stress depending upon two factors, i.e., (i) the value of Poisson's ratio and (ii) the relative density of the P/M preform in the case of the simple compression test were proposed in the literature.[18] However, copper-based materials are hard to form as they offer resistance to the forming load due to the formation of intermetallic compounds. Thus, it is essential to investigate the deformation behaviour of the Cu-TiB_2-based composite developed in the present work.

The deformation behaviours of Al matrix composites have been studied extensively. There are, however, few research reports on the deformation behaviour of Cu-TiB_2 composites. In the present paper efforts were made to make composites of Cu-TiB_2. The TiB_2 used is synthesized by using self-propagating high-temperature synthesis (SHS). Until now there is no report of workability studies on Cu-TiB_2 composites. The workability studies of the composites using a cold upsetting test are evaluated.

2 EXPERIMENTAL DETAILS

Cu-TiB_2 composite sintered preforms were selected in order to provide a reasonably wide range of study, namely, workability and work-hardening behaviour during cold upset operation. The commercially available copper powder was obtained from Alfa Aeser and the TiB_2 powder was produced using self-propagating high-temperature synthesis (SHS) in our lab, igniting the stoichiometric mixture of 20 g according to Equation (1), in a tubular furnace, maintaining an argon atmosphere. To investigate the particle size, shape and its distribution, copper, TiB_2 powders were studied using a scanning electron microscope (SEM) (**Figure 1**). The Cu-TiB_2 powders with different weight percentages of TiB_2, namely, 2 %, 4 % and 6 %, blend in a mortar mixer in order to obtain a homogeneous mixture.

The powders were compacted in a 25-ton manual pellet press with the closed die set assembly technique. Compacts of 15-mm diameter were prepared with aspect ratios of 0.50, 0.75 and 1. The aspect ratio is the ratio of the height to the diameter of the sample. The approxi-

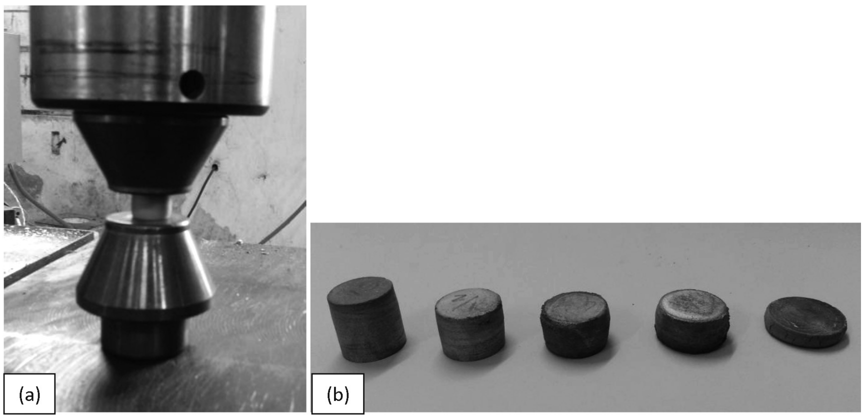

Figure 1: a) Upsetting test setup, b) deformed preforms
Slika 1: a) Sestav za krčilni preizkus, b) predoblike po deformaciji

mate initial preform density is 70 % of the theoretical density. These densities were achieved after sintering. Then the preforms were sintered in a tubular furnace at a temperature of 950 °C for a period of 1 h. To avoid oxidation the preforms were heated in an inert argon atmosphere. After the sintering schedule, the compacts were cooled in the furnace itself. The sintered preforms were cleaned and the dimensional measurement was made before the deformation.

The upsetting tests (**Figures 1a** and **1b**) were conducted on a hydraulic press having a capacity of 50 tons. Extreme care was taken to place the cylindrical specimen within the platens, concentric with the central axis of the hydraulic press (loading direction). Cylindrical preforms were cold upset between the flat platens. Each preform was subjected to an incremental compressive loading in steps until the appearance of visible cracks on the free surface.

Immediately after each incremental loading, the contact diameter at the top (D_{CT}), the contact diameter at the bottom (D_{CB}), the bulged diameter (D_B), the height of the preforms (h_f) and the density (ρ_f) were recorded. Before upsetting, the initial diameter (D_o), the initial height (h_o) and the initial preform density (ρ_o) of the specimens were measured. Moreover, the density measurements of the preforms were carried out using the Archimedes principle. Using the load, the dimensional parameters and density, the different true stresses (i.e., σ_z, σ_θ, σ_m and σ_{eff}) and the different true strains, (i.e., ε_z and ε_θ) and the workability parameters (β_σ) were determined using the expressions specified below for the triaxial stress-state condition.

For the present investigation, the TiB_2 powders were synthesized in-house as explained by the authors in a previous study.[19] The mixture of titanium oxide (TiO_2), boric acid (H_3BO_3) and magnesium was taken as per the stoichiometric reaction (Equation 1). The powders were mixed in a mortar mixer for about 20 min. A mixture of 20 g was then taken in a stainless-steel boat and was kept

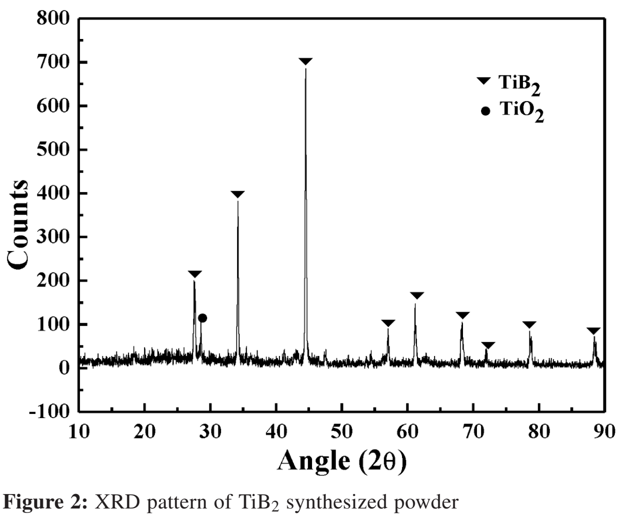

Figure 2: XRD pattern of TiB_2 synthesized powder
Slika 2: Rentgenogram sintetiziranega prahu TiB_2

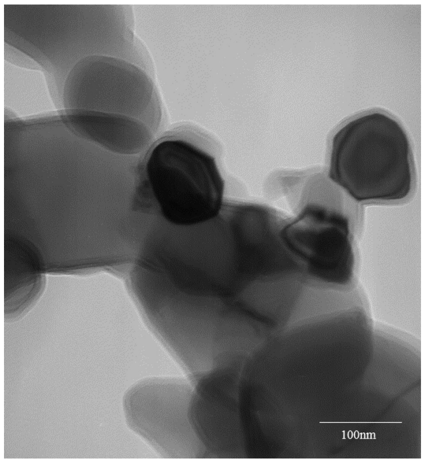

Figure 3: TEM image of TiB_2 synthesized powder
Slika 3: TEM-posnetek sintetiziranega prahu TiB_2

in a tubular furnace (Systems control, Chennai). The complete process was carried out in a highly pure argon atmosphere in order to maintain an inert atmosphere. The furnace was then heated up to 800 °C with a constant heating rate. It was observed that the reaction was taking place with an explosive sound at an approximate temperature of 680 ± 15 °C. The furnace is then left to cool to room temperature.

$$TiO_2\ (s) + 2H_3BO_3\ (s) + 5Mg\ (s) \rightarrow TiB_2\ (s) + MgO\ (s) + 3H_2O\ (g) + \Delta H \quad (1)$$

After cooling, the synthesized powder was taken out. It was observed that the reacted mixture is formed of black lumps, and some amount of white surface layer was seen on the lumps. The powder is then taken out and was crushed into fine powder before going to the leaching process, in order to make the leaching process effective. The leaching process was carried out in diluted HCl, with normality of 2 N. The solution was mixed

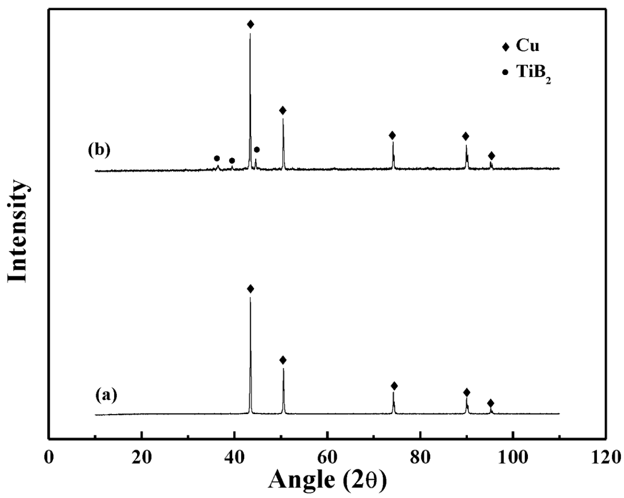

Figure 4: XRD patterns of samples: a) pure Cu and b) Cu-6 (6 % of mass fractions of TiB_2)
Slika 4: Rentgenograma vzorcev: a) čisti Cu in b) Cu-6 (6 % masnega deleža TiB_2)

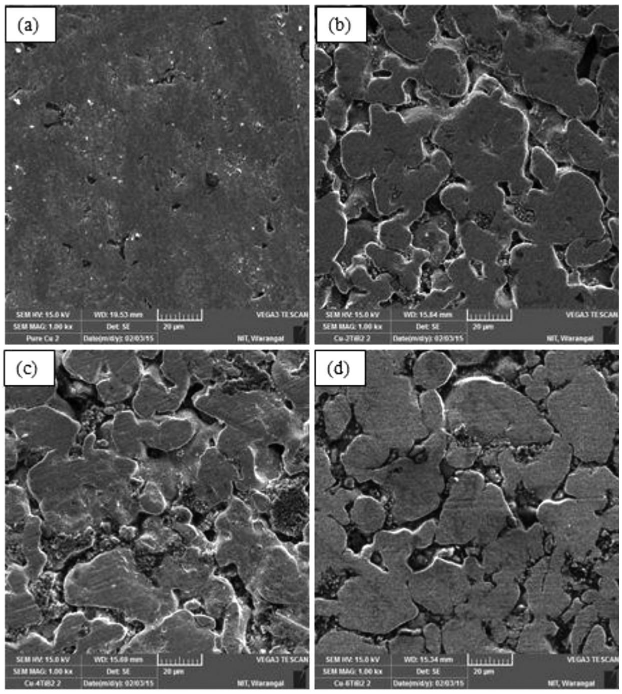

Figure 5: SEM images of: a) pure Cu, b) Cu-2 (2 % of mass fractions of TiB_2), c) Cu-4 (4 % of mass fractions of TiB_2), d) Cu-6 (6 % of mass fractions of TiB_2)

Slika 5: SEM-posnetek: a) čisti Cu, b) Cu-2 (2 % masnega deleža TiB_2), c) Cu-4 (4 % masnega deleža TiB_2), d) Cu-6 (6 % masnega deleža TiB_2)

with the crushed powder and heated up to 120 °C. The process was continued while the solution boils for about 10 min, and then the solution was separated using filter paper. The resulting powder, which was taken after the leaching process, was then dried in an oven for 1 h. The resulting powder is used in the present study.

The XRD patterns of the sample produced by the SHS process after leaching shows the presence of TiB_2 as major phase with TiO_2 as minor phase in **Figure 2**. The TEM image of the synthesized powder is shown in **Figure 3**. The TEM images show the formation of spherical and hexagonal TiB_2 particles.

The XRD pattern of pure Cu and Cu-6 (6 % of mass fractions of TiB_2) is shown in **Figure 4**. The pattern shows the presence of TiB_2 as small peaks and Cu as a major phase. This indicates there is no interaction between the Cu and TiB_2 during the pressureless sintering. It is because of the smaller weight percentage of TiB_2 in the Cu matrix.

The scanning electron microscope images of the Cu-TiB_2 samples are shown in **Figures 5a** and **5d**. Pure Cu is shown in **Figure 5a**. Cu-2 (2 % of mass fractions of TiB_2), Cu-4 (4 % of mass fractions of TiB_2) and Cu-6 (6 % of mass fractions of TiB_2) are shown in **Figures 5b** to **5d**, respectively. The SEM images reveal the surface morphology of the sintered samples. The images show the porosity, the distribution of the powder particles and the sintering behaviour.

3 THEORETICAL ANALYSIS

In the upsetting of P/M parts, the height decreases, the average density increases, and the various stresses increase.[20] The expressions for the normal stress (σ_z), normal strain (ε_z), hoop stress (σ_θ), hoop strain (ε_θ), hydrostatic stress (σ_m), effective stress (σ_{eff}), and effective strain (ε_{eff}) were taken from N. Selvakumar et al.[21] and Narayanasamy et al.[22]

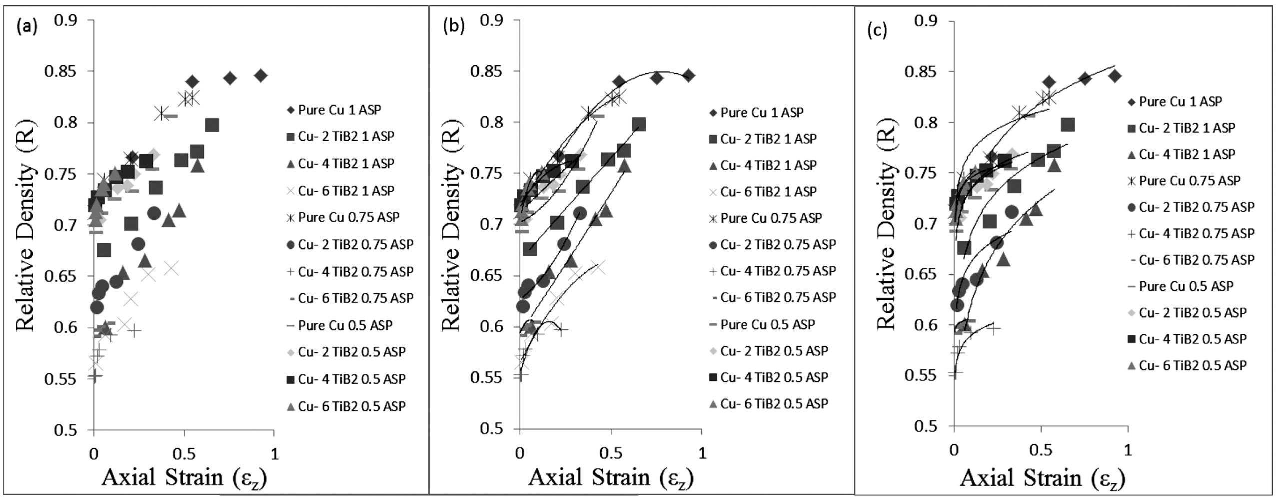

Figure 6: a) Relative density (R) versus axial strain (ε_z) for triaxial stress state condition, b) relative density (R) versus axial strain (ε_z) for triaxial stress-state condition (power-law curve-fitting results) and c) relative density (R) versus axial strain (ε_z) for triaxial stress-state condition (parabolic curve-fitting results)

Slika 6: a) Odvisnost relativne gostote (R) od osne napetosti (ε_z) pri triosnem napetostnem stanju, b) odvisnost relativne gostote (R) od osne napetosti (ε_z) pri triosnem napetostnem stanju (rezultati urejanja potenčne krivulje) in c) odvisnost relativne gostote (R) od osne napetosti (ε_z) pri pogoju triosnega napetostnega stanja (rezultati urejanja parabolične krivulje)

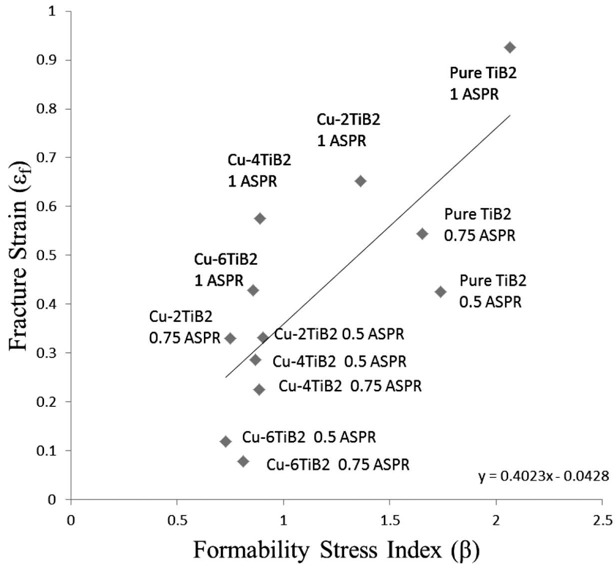

Figure 7: Fracture strain versus formability stress index (β)
Slika 7: Napetost loma v odvisnosti od indeksa preoblikovalne sile (β)

Triaxial Stress State Condition:

$$\alpha = \frac{A}{B} \tag{1}$$

$$A = (2+R^2)\sigma_\theta - R^2(\sigma_z + 2\sigma_\theta) \tag{2}$$

$$B = (2+R^2)\sigma_z - R^2(\sigma_z + 2\sigma_\theta) \tag{3}$$

$$\text{Hoop stress, } \sigma_\theta = \left[\frac{2\alpha + R^2}{2 - R^2 + 2R^2\alpha}\right]\sigma_z \tag{4}$$

$$\text{Hydrostatic stress, } \sigma_m = \frac{\sigma_z + 2\sigma_\theta}{3} \tag{5}$$

Effective stress,

$$\sigma_{eff} = \left[\frac{\sigma_z^2 + 2\sigma_\theta^2 - R^2(\sigma_\theta^2 + 2\sigma_z\sigma_\theta)}{2R^2 - 1}\right]^{0.5} \tag{6}$$

$$\text{Relative density, } R = \frac{\rho_f}{\rho_{th}} \tag{7}$$

ρ_f is the final density of the compact after deformation and ρ_{th} is the theoretical density of the compact.

$$\text{Formability Stress Index, } \beta = \frac{3\rho_m}{\sigma_{eff}} \tag{8}$$

4 RESULTS AND DISCUSSION

Figures 6a to **6c** show the relationship between the relative densities attained and the axial strain for the Cu-TiB_2 preforms. The compaction load was kept constant for all the samples compacted with different proportions of TiB_2 and copper. It is observed that the initial densification achieved is better for the preforms prepared with copper alone and its relative density is around 75 %. This reduces as the percentage of TiB_2 addition increases. The strain to failure was found to be low for the preforms with 6 % TiB_2 and it was found to increase as the TiB_2 decreases. Moreover, it can also be inferred that the strain to failure is low for the low initial relative densities.

A statistical curve-fitting technique was adopted for the drawn curves and the prediction equation developed from the curves was checked for its applicability by comparing the correlation coefficient 'R^2' values. These values can be used for modelling purposes and can also serve as prediction equations. In the present study, two

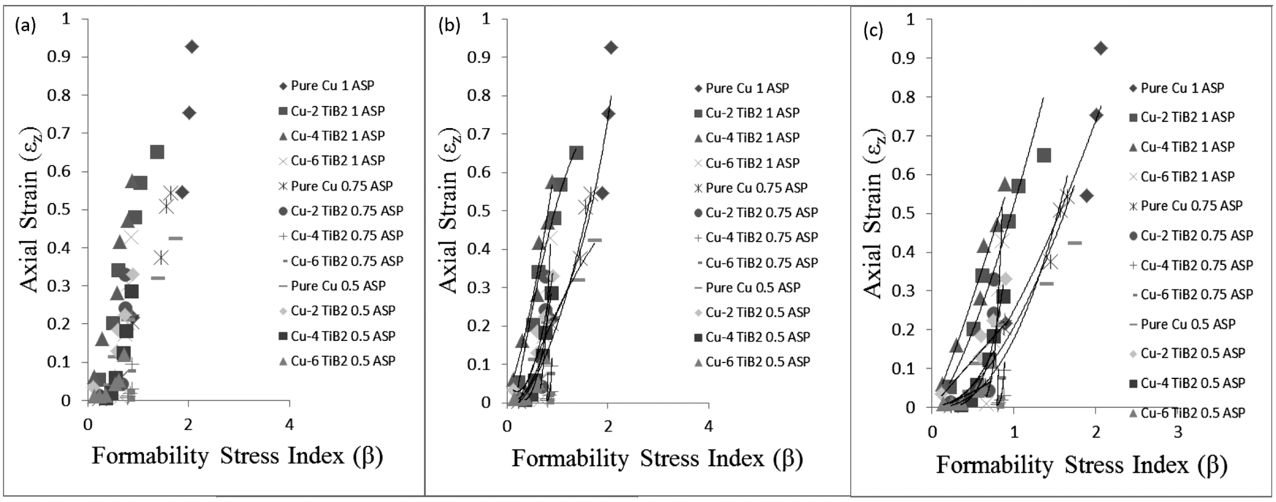

Figure 8: a) axial strain (ε_z) versus formability stress index (β) triaxial stress-state condition, b) axial strain (ε_z) versus formability stress index (β) triaxial stress-state condition (power-law curve-fitting results), c) axial strain (ε_z) versus formability stress index (β) triaxial stress-state condition (parabolic curve-fitting results)

Slika 8: a) odvisnost osne napetosti (ε_z) od indeksa preoblikovalne napetosti (β) pri triosnem napetostnem stanju, b) odvisnost osne napetosti (ε_z) od indeksa napetosti preoblikovanja (β) pri triosnem napetostnem stanju (rezultati urejanja potenčne krivulje), c) odvisnost osne napetosti (ε_z) od indeksa preoblikovalne napetosti (β) pri triosnem napetostnem stanju (rezultati urejanja parabolične krivulje)

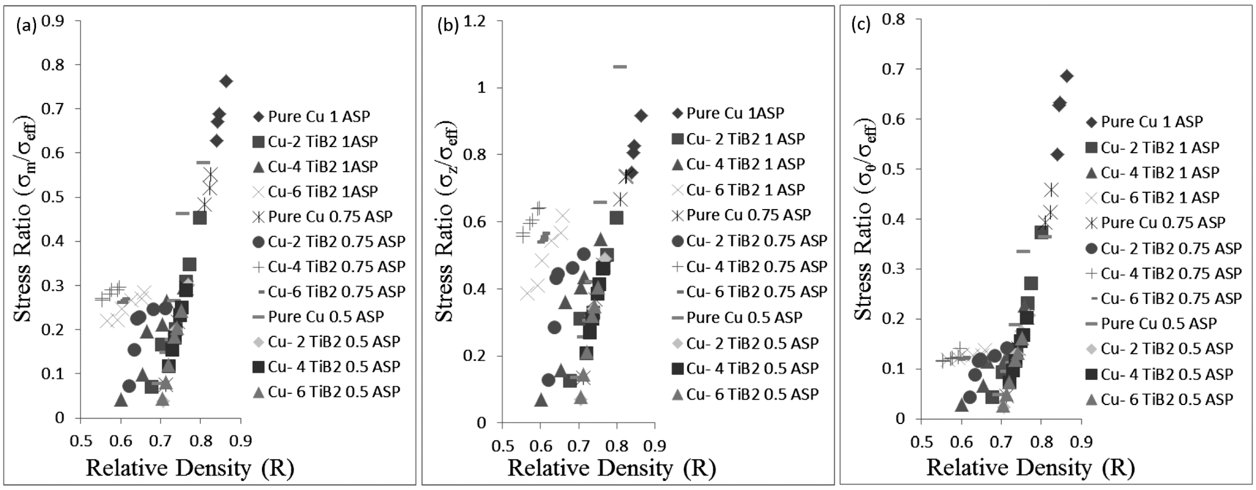

Figure 9: a) Stress ratio (σ_m/σ_{eff}) versus relative density (*R*), b) stress ratio (σ_z/σ_{eff}) versus relative density (*R*), c) stress ratio ($\sigma_\theta/\sigma_{eff}$) versus relative density (*R*)

Slika 9: a) Odvisnost razmerja napetosti (σ_m/σ_{eff}) od relativne gostote (*R*), b) odvisnost razmerja napetosti (σ_z/σ_{eff}) od relativne gostote (*R*), c) odvisnost razmerja napetosti ($\sigma_\theta/\sigma_{eff}$) od relativne gostote (*R*)

different curve-fitting techniques, i.e., the power law and parabolic curve fitting, were used.

As the aspect ratio increases, the fracture strain increases (**Figure 7**). The fracture strain decreases with the addition of TiB_2. Irrespective of the TiB_2 content, the fracture strain is less for 0.5 aspect ratio preforms. The decrease in the fracture strain indicates that the composite has attained a higher strength level with the addition of TiB_2, with less sacrifice in the strain values. The addition of TiB_2 to a preform with an aspect ratio of 1 has increased the strength with very little loss of fracture strain.

Figures 8a to **8c** show the plot drawn between the axial strain and the formability stress index (b). A statistical fit is made using the polynomial function and the power-law function. It is found that the power law related the parameters with higher accuracy. The addition of TiB_2 decreased the strain further.

For preforms with a higher aspect ratio and a lower initial relative density, the formability stress-index value moves closer to the minimum value. The reason is that this preform contains more pores and the porous bed height is larger or greater. The increase in relative density with increasing deformation is less in this case compared to lower aspect ratio preform. A parabolic curve-fitting technique was applied to relate the formability stress index and the axial strain for a varying aspect ratio and relative density. The polynomial equations obtained for each aspect ratio and relative density along with its regression co-efficient value are presented in **Table 1**, where it is observed that the constant value decreases with a decreasing amount of relative density, irrespective of the aspect ratio.

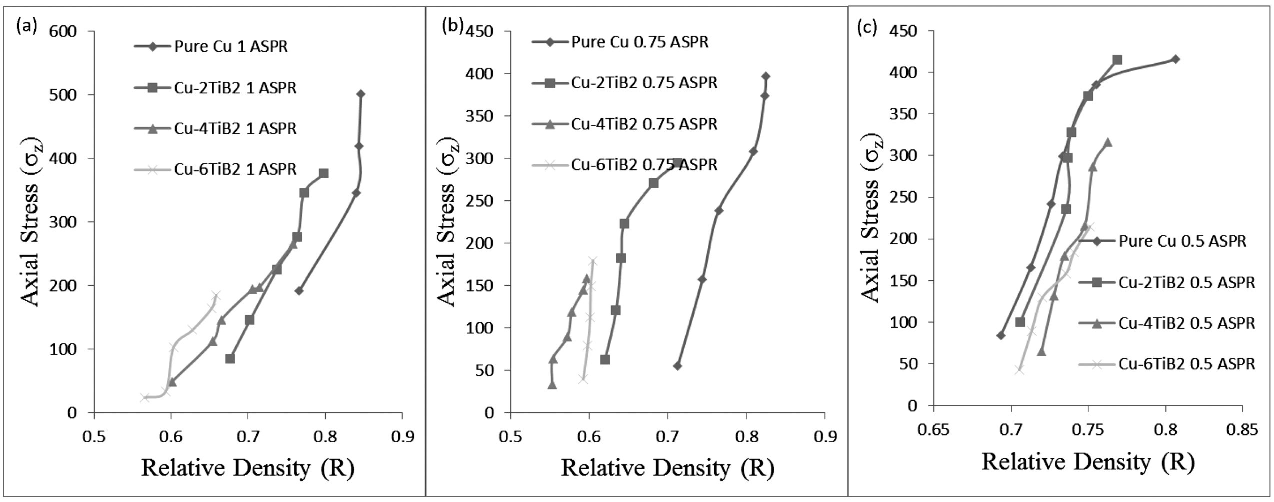

Figure 10: Axial stress (σ_z) versus relative density (*R*): a) 1 ASPR, b) 0.75 ASPR and c) 0.5 ASPR

Slika 10: Odvisnost osne napetosti (σ_z) od relativne gostote (*R*): a) 1 ASPR, b) 0,75 ASPR in c) 0,5 ASPR

Table 1: Parabolic curve-fitting equations and R^2 values
Tabela 1: Enačbe urejanja parabolične krivulje in vrednosti R^2

Sample	Aspect ratio	Equation	R^2 value
Pure Cu	1	$y = -0.2603x^2 + 0.4053x + 0.6916$	0.9863
Cu-2%TiB_2		$y = -0.0045x^2 + 0.2031x + 0.6646$	0.9915
Cu-4%TiB_2		$y = 0.0187x^2 + 0.2652x + 0.5934$	0.9671
Cu-6%TiB_2		$y = -0.307x^2 + 0.3572x + 0.5642$	0.9506
Pure Cu	0.75	$y = -0.2038x^2 + 0.312x + 0.7167$	0.9804
Cu-2%TiB_2		$y = 0.3857x^2 + 0.1301x + 0.6268$	0.9724
Cu-4%TiB_2		$y = -2.0138x^2 + 0.645x + 0.5534$	0.8919
Cu-6%TiB_2		$y = -4.1476x^2 + 0.4749x + 0.593$	0.9105
Pure Cu	0.5	$y = 0.3627x^2 + 0.079x + 0.7022$	0.9525
Cu-2%TiB_2		$y = -0.0329x^2 + 0.1792x + 0.7117$	0.8193
Cu-4%TiB_2		$y = -0.4124x^2 + 0.2648x + 0.72$	0.9889
Cu-6%TiB_2		$y = -4.6848x^2 + 0.9689x + 0.702$	0.9444

Figures 9a to **9c** give the plot of the relative density with the stress ratio. The change of density along the axial and hoop stress directions was analysed. **Figure 8a** shows the variation of the relative density with the mean stress ratio. It is found that Cu with 4 % TiB_2 and an aspect ratio of 0.5 yielded high density values with a high load-bearing capacity. The same was true for the axial stress ratio and the hoop stress ratio. The hoop stress is responsible for the initiation of cracks in the preforms. Thus, it is clear that the addition of 4 % TiB_2 improves the density of the preforms and postpones the initiation of cracks. As the relative density increases the stress ratio parameter also increases.

It was found that the relative density increases as the stress-ratio parameter increases. The effect of the aspect ratio on the stress-ratio parameter is found to be minimal for the lower initial preform density preforms. However, as the initial preform density increases, a higher stress ratio parameter is observed for higher initial preform densities with a lower aspect ratio. This shows that the formability increases for the preforms with lower aspect ratios and higher initial preform densities.

The **Figures 10a** to **10c** show plots of the axial stress (σz) against the relative density R. The experiment was done with preforms that have initial densities ranging from 0.6 to 0.75 and aspect ratios ranging from 0.5 to 1. The axial stress is found to increase rapidly during the initial stage of densification, and thereafter continue to increase with a lesser rate. The increase in stress due to the forming load is followed by the closure of pores in the preform, leading to its densification. This densification is attributed to the combined effect of the geometric and the matrix work-hardening. The preforms with a lower TiB_2 content were found to attain a higher stress value than the TiB_2 preforms. Along with the densification, the load-bearing capability of the preforms also increases, as is evident from the higher stress values in the plot (**Figures 10**a to **10c**).

It was found that the preform with 6 % TiB_2 and a 0.5 aspect ratio densified more. Preforms with a high initial preform density had a higher load-bearing capacity and a longer strain to failure. This is due to the presence of a smaller number of pores. At the same time, the dislocation density increases rapidly during plastic deformation, thereby resulting in a steep axial stress regime with a smaller increase in the corresponding relative density.

5 CONCLUSION

The formability behaviours of sintered Cu-TiB_2 composite preforms was studied. The formability stress index increased with an increase in the initial preform fractional density and decreased with the aspect ratios. A statistical fitting method was performed on the curve drawn between the axial strain and the stress formability index, and the parabolic curve fitting was found to give better predictive results. For the compacts with a higher value of the aspect ratio and initial preform density, the initiation of the crack appeared at a very high fracture strain.

Acknowledgement

This research work has been funded by the Council of Scientific and Industrial Research (CSIR) (sanction letter no. 22/597/12-EMR-II, dated 25/03/2012).

6 REFERENCES

[1] J. Mascarenhas, Powder metallurgy: a major partner of the sustainable development, Materials Science Forum, 455–456 (**2004**), 857–860, doi:10.4028/ www.scientific.net/ MSF.455-456.857

[2] G. E. Dieter, Mechanical Metallurgy, 3rd ed., McGraw-Hill, New York 1981

[3] T. J. Griffiths, R. Davies, M. B. Bassett, Compatibility equations for the powder forging process, Powder Metallurgy, 4 (**1977**), 214–220

[4] E. Bilgi, H. Erdem Çamurlu, B. Akgün, Y. Topkaya, N. Sevinç, Formation of TiB_2 by volume combustion and mechanochemical process, Mater. Res. Bull., 43 (**2008**), 873–881, doi:10.1016/ j.materresbull.2007.05.001

[5] A. Nekahi, S. Firoozi, Effect of KCl, NaCl and CaCl2 mixture on volume combustion synthesis of TiB_2 nanoparticles, Materials

Research Bulletin, 46 (**2011**) 9, 1377–1383, doi:10.1016/ j.materresbull.2011.05.013

[6] T. S. Srivatsan, G. Guruprasad, D. Black, R. Radhakrishnan, T. S. Sudarshan, Influence of TiB_2 content on microstructure and hardness of TiB_2 – B_4C composite, Powder Technology, 159 (**2005**), 161–167, doi:10.1016/j.powtec.2005.08.003

[7] X. K. Sun, S. J. Chen, J. Z. Xu, L. D. Zhen, K. T. Kim, Analysis of cold compaction densification behaviour of metal powders, Materials Science and Engineering, A267 (**1999**), 43–49, doi:10.1016/S0921-5093(99)00052-0

[8] H. A. Kuhn, C. L. Downey, How flow and fracture affect design of preforms for powder forging, International Journal of Powder Metallurgy and Powder Technology, 10 (**1974**) 1, 59–66

[9] I. Pokorska, Deformation of powder metallurgy materials in cold and hot forming, Journal of Materials Processing Technology, 196 (**2008**) 1–3, 15–32, doi:10.1016/ j.jmatprotec.2007.08.017

[10] P. W. Taubenblat, Importance of copper in powder metallurgy, International Journal of Powder Metallurgy, 39 (**2003**), 25–28

[11] R. Narayanasamy, V. Anandakrishnan, K. S. Pandey, Some aspects on plastic deformation of copper and copper–titanium carbide powder metallurgy composite preforms during cold upsetting, International Journal of Material Forming, 1 (**2008**) 4, 189–209, doi:10.1007/s12289-008-0383-7

[12] M. Sumathi, N. Selvakumar, R. Narayanasamy, Workability studies on sintered Cu-10SiC preforms during cold axial upsetting, Materials and Design, 39 (**2012**), 1–8, doi:10.1016/j.matdes.2012.02.004

[13] S. Narayan, A. Rajeshkannan, Workability studies in forming of sintered Fe-0.35C powder metallurgy preform during cold upsetting, Journal of Iron and Steel Research International, 18 (**2011**), 71–78, doi:10.1016/S1006-706X(12)60012-0

[14] G. Dieter, Handbook on workability analysis and applications, ASM publications 1, 2002

[15] R. Narayanasamy, V. Anandakrishnan, K. S. Pandey, Effect of carbon content on workability of powder metallurgy steels, Materials Science and Engineering A, 494 (**2008**), 337–342, doi:10.1016/ j.msea.2008.04.022

[16] M. Abdel-Rahman, E. Sheikh, Workability in Forging of Powder Metallurgy Compacts, Journal of Materials Processing Technology, 54 (**1995**), 97–102

[17] J. J. Park, Constitutive relations to predict plastic deformations in porous metal during Compaction, International Journal of Mechanical Sciences, 37 (**1995**), 709–719

[18] R. Narayanasamy, R. Ponalagusamy, A Mathematical theory of plasticity for compressible powder metallurgy materials – Part II, Journal of Materials Processing Technology, 97 (**2000**), 110–113, doi:10.1016/S0924-0136(99)00357-X

[19] S. Gadakary, A. K. Khanra, R. Veerababu, Production of nanocrystalline TiB_2 powder through self-propagating high temperature synthesis (SHS) of TiO_2–H_3BO_3–Mg mixture, Advances in Applied Ceramics, 113 (**2014**) 7, 419-426, doi:10.1179/1743676114Y. 0000000188

[20] R. Narayanasamy, T. Ramesh, K. S. Pandey, S. K. Pandey, Effect of particle size on new constitutive relationship of aluminium–iron powder metallurgy composite during cold upsetting, Material and Design, 29 (**2008**), 1011–1026, doi:10.1016/j.matdes.2006.06.004

[21] N. Selvakumar, R. Narayanasamy, Phenomenon of strain hardening behaviour of sintered aluminium preforms during cold axial forming, Journal of Materials Processing Technology, 142 (**2003**), 347–54, doi:10.1016/S0924-0136(03)00605-8

[22] R. Narayanasamy, T. Ramesh, K. S. Pandey, Some aspects on workability of aluminium–iron powder metallurgy composite during cold upsetting, Materials Science and Engineering, A391 (**2005**), 418–426, doi:10.1016/j.msea.2004.09.018